Proceedings of the 2nd Marine Energy Technology Symposium
METS2014
April 15-18, 2014, Seattle, WA

WAVE PERIOD RATIOS AND THE CALCULATION OF WAVE POWER

Brendan Cahill [1]
Oregon State University
Corvallis, OR, U.S.A.

Tony Lewis
Beaufort Research, University College Cork
Cork, Ireland

[1]Brendan.Cahill@fulbrightmail.org

ABSTRACT

An informed, and accurate, characterization of the wave energy resource is an essential aspect selection of suitable sites for the first commercial installations of wave energy converters. This paper describes a detailed study on the variability of wave climate and measured spectral shapes and how they differ from the standard formulations prescribed by theory. In particular dissonance between the ratio of the energy period (T_E) to the average zero-crossing period (T_{02}) is investigated at a range of open ocean locations. This relationship is important in the context of resource assessment as many previous works, lacking in detailed spectral data, have often assumed an incorrect ratio. This in turn has influenced the accuracy of the resulting estimates of wave energy. It is demonstrated that the earlier use of the frequently-employed wave period ratios is erroneous and more suitable relationships are presented for the Bretschneider and JONSWAP theoretical spectra. Furthermore, analysis of measured buoy data from real sea-states is used to illustrate that this relationship can in fact vary significantly in practice, depending on geographical location and the prevalent wave conditions. The variability that exists in spectral shape and bandwidth, and the effect this has on the relationship between T_E and T_{02}, is illustrated through the comparison of recorded spectra with the Bretschneider spectrum. Analysis of a fifteen year dataset measured by a buoy off the coast of Southern California is presented to illustrate how the wave period ratio fluctuates on a seasonal and interannual basis, while it is also shown that previous studies of the Irish wave energy resource may have underestimated the theoretical power available by as much as 18%.

INTRODUCTION

Characterizing the wave energy resource in locations where there is a scarcity of quality wave measurements particularly spectral data necessitates the need for assumptions based on theory to be made in order to infer some of the required parameters. For example, the Irish M-Buoy network managed by the Marine Institute provides values for the average zero-crossing period (T_z or T_{02}) but in the context of wave energy resource assessment parameters such as the peak period (T_p), the energy period (T_E), and increasingly the mean period (T_{01}) are used more frequently. Wave models may suffer from similar shortcomings if their outputs are constrained to a reduced range of parameters in an effort to decrease computation time.

For regular sea states, in deep water, the power per unit width of wave crest, P, is given by Equation 1, where H_{m0} is the significant wave height.

$$P = 0.49 H_{m0}^2 T_E \qquad (1)$$

In order to determine the necessary T_E values from limited datasets it has been common practice to employ fixed conversion factors based on a theoretical spectral shape, such as Bretschneider or JONSWAP, which is deemed to be representative of the dominant local wave conditions. As a result, assessments of wave energy resource which rely on this approach are sensitive to inaccuracies if the incorrect relationship between parameters is assumed or if the spectral shape considered characteristic for the data is inappropriate.

An illustration of how an unsuitable assumption can result in imprecision in the calculation of the available wave power is contained in the Accessible Wave Energy Resource Atlas [1], the standard reference for Ireland's potential resource. In this study the theoretical wave energy resource was calculated from the summary statistics H_{m0} and T_{02}, generated from a WAM forecast model, as well as from the M-Buoys deployed around the coast, using the formula

$$P = 0.55 H_{m0}^2 T_{02} \qquad (2)$$

which is based on Equation 1 under the assumption that T_E/T_{02}=1.12. This relationship will henceforth be referred to as the wave period ratio (WPR) for the remainder of this paper. To the best of the authors' knowledge the first published reference to this form of the equation is contained in an early review of wave energy research [2] which assumes that all measured records in a dataset can be represented by the Bretschneider spectrum. This formula has since been reproduced in other works [3–5], as well as in the Irish Wave Atlas. A number of other studies [6,7]—which also assume a Bretschneider spectral shape for the records being analyzed—use a slightly different WPR, with T_E/T_{02}=1.14. The JONSWAP spectrum is considered representative in the assessment of the wave energy resource of the United Kingdom [8] and period ratio values ranging from 1.06-1.14 are employed, depending on the magnitude of the model-derived wave period and whether the sea-state is dominated by a swell or wind-sea system.

The prevalence of these disparate values of WPR can be a source of confusion and inaccuracy. This uncertainty can potentially influence both the calculation of the theoretical resource and also the estimation of WEC output from power matrices; many of these require values of T_E as an input. The growing availability of spectral measurements, and the development of standards to allow for the correct interpretation of these data [9–11], should remove any ambiguity associated with the calculation of wave power. In cases where the available data are limited, however, the application of a user defined WPR is unavoidable so an improved level of precision is required. It is with this consideration in mind that the research presented here was undertaken.

In this paper it is demonstrated that the use of the frequently-employed wave period ratios cited earlier is erroneous and more suitable relationships are presented for the Bretschneider and JONSWAP theoretical spectra. Furthermore, analysis of measured buoy data from real sea-states is used to illustrate that this relationship can in fact vary significantly in practice, depending on geographical location and the prevalent wave conditions. Analysis of a fifteen year dataset measured by a buoy off the coast of Southern California is presented to illustrate how the WPR fluctuates on a seasonal and interannual basis. The variability that exists in spectral shape and bandwidth, and the effect this has on the relationship between T_E and T_{02}, is illustrated through the comparison of recorded spectra with the Bretschneider spectrum. The results presented here will allow for more accurate use to be made out of limited datasets such as the measurements produced by the M-Buoy network.

WAVE PERIOD RATIO OF STANDARD SPECTRAL SHAPES

As discussed in the previous section, some studies of wave energy resource rely on theoretical spectral formulations to infer more detailed information from the available summary statistics where there is an absence of measured spectral or surface elevation data. Several standard spectral shapes have been derived to describe sea-states by applying fitting techniques to empirically collected data. In this section two commonly used spectra in wave energy research—the Bretschneider spectrum and the JONSWAP spectrum—are analyzed and the ratios of T_E/T_{02} that can be expected from them are compared to the values used in the references cited previously.

Bretschneider Spectrum

In order to derive the WPR for the Bretschneider Spectrum a constant, α_B, is introduced to represent the relationship between the energy period, T_E, and the zero-crossing period, T_{02}:

$$T_E = \alpha_B T_{02} \qquad (3)$$

This relationship can then be rewritten in terms of spectral moments.

$$\frac{m_{-1}}{m_0} = \alpha_B \sqrt{\frac{m_0}{m_2}} \qquad (4)$$

Following Tucker and Pitt [12], the n^{th} spectral moment, m_n, can be stated in terms of constants A and B by applying Equation 5. This allows the m_{-1}, m_0 and m_2 in Equation 4 to be rewritten in terms of A and B, as shown in Equation 6.

$$m_n = \frac{1}{4} A B^{\left(\frac{n}{4}\right)-1} \Gamma[1-(n/4)] \qquad (5)$$

$$\frac{0.2266\frac{A}{B^{\frac{5}{4}}}}{\frac{A}{4B}} = \alpha_B \sqrt{\frac{\frac{A}{4B}}{0.443\frac{A}{\sqrt{B}}}} \qquad (6)$$

Equation 6 can be manipulated to show that α_B=1.206. Thus, for a Bretschneider Spectrum the WPR is given by

$$T_E = 1.206 T_{02} \qquad (7)$$

This indicates that the assumptions that the WPR for the Bretschneider spectrum is either 1.12 or 1.14 are inaccurate. By substituting Equation 7 into Equation 1 it is possible to calculate the average wave power using the summary statistics H_{m0} and T_{02}.

$$P = 0.59H_{m0}^2 T_{02} \quad (8)$$

If this is compared to Equation 2, which assumed a T_E/T_{02} ratio of 1.12 for the Bretschneider Spectrum, it is possible to conclude that studies which assumed the incorrect WPR value, such as the Accessible Wave Energy Resource Atlas [1], underestimated the available wave power by approximately 7% if the Bretschneider spectrum is considered to be representative of the prevalent conditions.

JONSWAP Spectrum

Following the approach used previously for the Bretschneider Spectrum it is possible to derive a wave period ratio (α_J) between the energy period, T_E, and the zero-crossing period, T_{02}, for a JONSWAP Spectrum.

$$T_E = \alpha_J T_{02} \quad (9)$$

Equation 9 is restated in terms of spectral moments in Equation 10.

$$\frac{m_{-1}}{m_0} = \alpha_J \sqrt{\frac{m_0}{m_2}} \quad (10)$$

As with Equation 6, the spectral moment terms in Equation 10 are rearranged, in this case in terms of H_{m0}, the peak frequency f_p and the peak shape parameter γ. These alternative approximations of m_{-1}, m_0 and m_2 for the JONSWAP spectrum are taken from [13] and are reproduced in Equations 11-13.

$$m_{-1} = \frac{1}{32\pi} H_s^2 f_p^{-1} \frac{4.2+\gamma}{5+\gamma} \quad (11)$$

$$m_0 = \frac{1}{16} H_s^2 \quad (12)$$

$$m_2 = \frac{\pi^2}{4} H_s^2 f_p^2 \frac{11+\gamma}{5+\gamma} \quad (13)$$

Equation 10 is rewritten with these substitutions and is simplified in stages, which allows α_J to be written in terms of γ in Equation 14.

$$\alpha_J = \left(\frac{4.2+\gamma}{5+\gamma}\right).\left(\frac{11+\gamma}{5+\gamma}\right)^{\frac{1}{2}} \quad (14)$$

TABLE 1. T_E/ T_{02} WAVE PERIOD RATIOS FOR JONSWAP SPECTRA.

γ	WPR (α_J)
1	1.22
2	1.20
3.3	1.18
5	1.16
7	1.14
10	1.12

By applying Equation 14 the WPR value for a JONSWAP Spectrum is given in Table 1 for a range of γ values. It is noticeable that as expected the wave period ratio is similar to that of the Bretschneider spectrum when γ=1. The WPR decreases as the peaks of the spectra become more pronounced. Table 1 also indicates that it is possible to generate spectra with WPR values of 1.12 and 1.14 which were cited previously using the JONSWAP formula, however to do so requires γ to equal 10 and 7 respectively. It has been shown [14] that γ follows a normal distribution with a mean of 3.3 and a standard deviation of 0.79. This suggests that such high values of γ are unlikely to occur in the ocean. Therefore, the corresponding WPRs are unrepresentative of real sea states and so should be considered inaccurate.

WAVE PERIOD RATIO IN REAL SEAS

As the results detailed in the previous section relate only to the case of theoretical spectra, analysis of measured wave data, collected at a number of different water depths and geographical locations, was carried out, and is detailed in the following sections in order to assess how applicable the theoretical WPR of 1.2 derived previously for the Bretschneider Spectrum is to real sea-states.

Measured Wave Data

The nature of the WPR in real seas was analysed using measurements obtained from four geographical regions: the west coast of Ireland; the eastern seaboard of the United States; and the states of Oregon and California on the US Pacific coast. Data from Irish waters were obtained from the Datawell Waverider buoys stationed at the Atlantic Marine Energy Test Site (AMETS), off Belmullet, Co. Mayo, and deployed near Loop Head, Co. Clare during a previous measurement campaign [15]. Data from the United States were obtained through the websites of the National Data Buoy Centre and the Scripps Institute of Oceanography.

Average Annual Values of WPR

Measured spectral data was processed and analyzed for each location, rather than relying on archived values of the summary statistics of interest. Spectral moments and important wave parameters were derived from the observed spectra. The characteristic WPR for each location is defined in Equation 15 as the average value of T_E/T_{02}.

$$WPR = \frac{1}{N}\sum_{i=1}^{N}\frac{(T_E)_i}{(T_{02})_i} \quad (15)$$

The details of the datasets and the computed WPRs for the various regions that were studied are compiled in Tables 2-5. Data analyzed in this section were obtained from a number of different types of measurement buoy, primarily surface following Datawell Waverider buoys and the 3m diameter Pitch-Roll-Heave buoys operated by the NDBC. Where possible, a full year's worth of data was analyzed at each location to prevent seasonal bias affecting the results. Unfortunately there is poor data availability during the summer months for the Belmullet and Loop Head buoys.

TABLE 2. WAVE PERIOD RATIOS FOR IRISH SITES.

Location	WPR
AMETS	1.32
Loop Head	1.33

TABLE 3. WAVE PERIOD RATIOS FOR US EAST COAST SITES (2010).

NDBC Station	Location	WPR
41001	Nantucket, MA	1.205
44008	Cape Hatteras, NC	1.207
44014	Virginia Beach, VA	1.244
41048	West of Bermuda	1.208

TABLE 4. WAVE PERIOD RATIOS FOR OREGON SITES (2010).

NDBC Station	Location	WPR
46029	Colorado River	1.274
46089	Tillamook	1.260
46050	Stonewall Bank	1.263
46266	Umpqua	1.299

TABLE 5. WAVE PERIOD RATIOS FOR CALIFORNIA SITES (2010).

NDBC Station	Location	WPR
46028	San Francisco	1.295
463298	Point Sur	1.346
46028	Cape San Martin	1.273
46215	Diablo Canyon,	1.378

It is evident that distinct ranges of the T_E/T_{02} ratio are associated with each of the geographical regions that were studied. The average values of T_E/T_{02} calculated from buoy data measured off the Atlantic coast of the United States can be seen to agree quite well with the Bretschneider approximation. Most of the datasets from this region which were analyzed were found to have values close to 1.2, though a value of 1.24 was calculated for the Virginia Beach buoy. It is noticeable that the range of values from the Pacific coast conforms poorly to what is expected from the theoretical spectra. The WPRs for the Oregon buoys lie in the range 1.26-1.30, while to their south the locations off the Californian exhibit higher ratios (1.27-1.38) with a greater degree of variation between sites.

The WPRs derived from measurements at the exposed Atlantic sites in Ireland—AMETS and Loop Head—are 1.32 and 1.35 respectively. This is significant in the context of wave energy resource assessment and economic modelling when one considers that, as mentioned previously, a value of 1.12 has often been assumed. If the WPR derived from the AMETS and Loop Head observations were considered to be characteristic for the entire Irish western seaboard the magnitude of the theoretical wave energy resource presented in the Accessible Wave Energy Atlas could be revised upwards by 18%. Similar analysis could be carried out for other wave period parameters. For example T_p is often included in limited datasets. The T_E/T_P ratio for a Bretschneider spectrum is 0.85 while an average value of 0.83 is derived from the measured data from Belmullet.

Temporal Variability of WPR

Annual average values were used in the previous section to characterize the expected WPR at the locations being analyzed. In reality this relationship is transient and its values can fluctuate significantly at a site depending on the incident wave conditions and the composition of the wave spectra. This variability is illustrated in Figure 1 which plots the evolution of the WPR and the significant wave height measured by the Datawell Waverider at the 50 m depth at AMETS in January 2011.

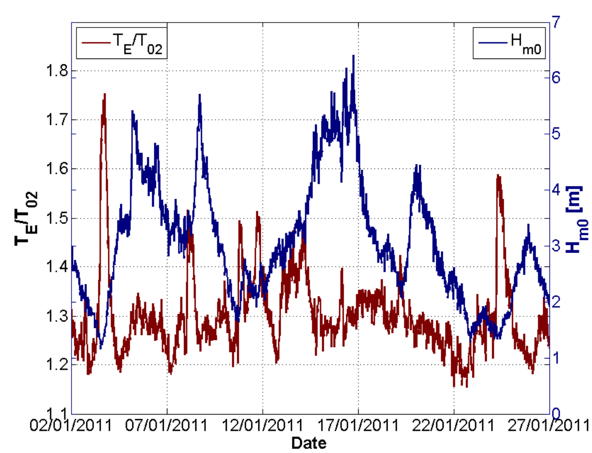

FIGURE 1. TIME SERIES OF WAVE PERIOD RATIO AND H_{M0} FROM AMETS (JANUARY 2011).

Figure 1 highlights that the WPR is not a static quantity and that it is loosely correlated to H_{m0}; in general T_E/T_{02} is higher in low sea-states, and vice versa. This relationship is also evident in Figure 2- where the WPR is plotted against the corresponding H_{m0} values for a dataset of one full year. It is evident that large discrepancies exist in the relationship between T_E and T_{02} when the significant wave height is low and that the highest WPR values tend to occur during these frequently occurring conditions. Conversely, WPRs are constantly closer to the value of 1.2 derived from the Bretschneider spectrum during the greater sea-states.

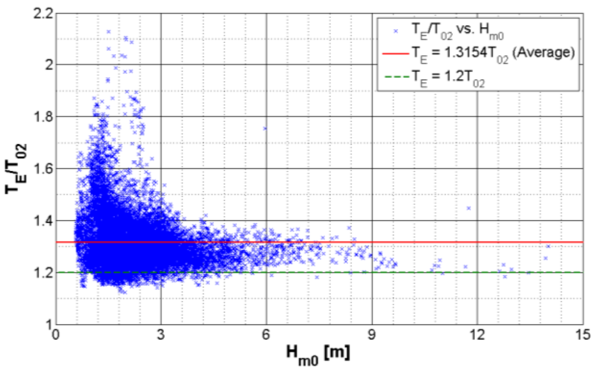

FIGURE 2. WAVE PERIOD RATIO PLOTTED AGAINST H_{M0} FOR AMETS.

Seasonal Variability

Wave conditions are known to exhibit variability over seasonal, interannual and decadal time scales. The possibility of the WPR displaying long term trends was investigated in order to assess whether any variations should be considered significant over the lifetime of a WEC development. Due to the lack of records of sufficient duration from the buoys off the Irish coasts a 15 year dataset of measurements (1997-2011) taken from NDBC Buoy 46215 located near Diablo Canyon in Southern California was analyzed. In Table 4 it was noted that the average WPR calculated for this location for the year 2010 was 1.378.

Rolling averages of T_E/T_{02} and wave power were computed, with a window length of one month, and the results illustrated in Figure 3. The strong seasonal trends in wave power are evident, with well-defined peaks for each winter period and corresponding troughs in the summer months, though the plots of the period ratio tend not to follow as smooth a profile. Visual inspection of Figure 3 suggests that in general peaks of wave power coincide with lower value of T_E/T_{02}, though instances where the opposite is true are also evident. This is confirmed by statistical checks which indicate that there is a small degree of negative correlation (-0.24) between the two series.

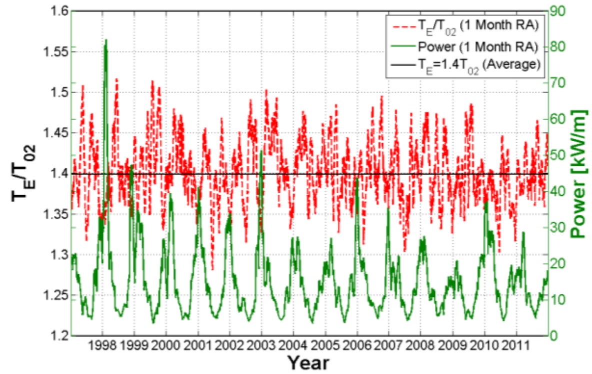

FIGURE 3. ONE MONTH ROLLING AVERAGE OF WAVE PERIOD RATIO AND WAVE POWER (1997-2011).

Interannual Variability

The average annual values of wave period for each of the 15 years of available data were computed from the measured wave spectra. The results are illustrated in Figure 4. These values of the WPR range from 1.37 to 1.41, a percentage difference of approximately 3%. The overall average figure for the 15 year period was 1.4. The average values of the WPR are also plotted against the annual average annual wave power for each year in Figure 5 While the previous analyses indicated that individual sea-states with low values of T_E/T_{02} are associated with increasing wave power there is no discernable trend apparent when annual averages are assessed, with the most energetic years displaying a wide spread of values.

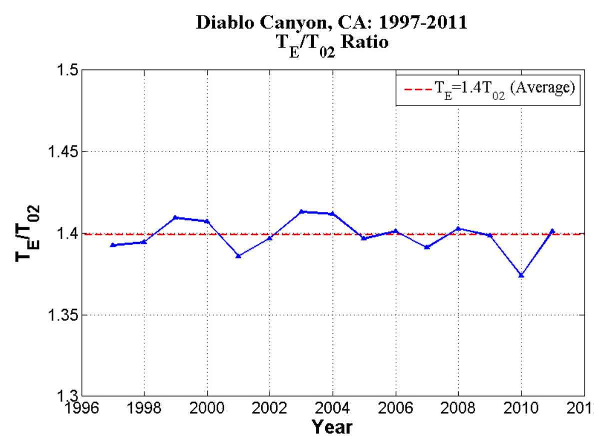

FIGURE 4. ANNUAL AVERAGE WAVE PERIOD RATIO FOR DIABLO CANYON BUOY (1997-2011).

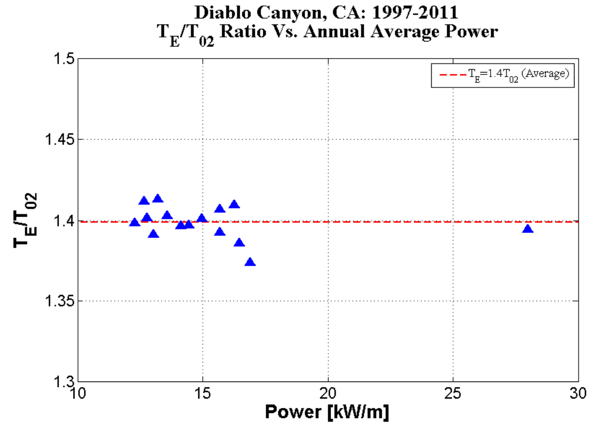

FIGURE 5. ANNUAL AVERAGE WAVE PERIOD RATIO VS. ANNUAL AVERAGE WAVE POWER FOR DIABLO CANYON (1997-2011).

SPECTRAL VARIABILITY AND WPR

Previous work has demonstrated the effect that altering the distribution of standard spectral shapes across the frequency scale has on the WPR [16]. The following sections address the influence that spectral shape, including the presence of multiple peaks, has on the T_E/T_{02} relationship through the analysis of measured data from open ocean sites.

Multi-Modal Spectra

The spectra from four of the outlier points in Figure 2 for the AMETS data are plotted against their equivalent Bretschneider spectrum in Figure 6. Two of the most noticeable outliers—the points with H_{m0} of 5.95 m and 11.75 m, and T_E/T_{02} equal to 1.76 and 1.45 respectively—are included as they present particularly interesting cases. An obvious similarity is apparent, with multiple peaks evident in the measured spectra and the primary peaks occurring at lower frequencies than the peaks of the corresponding Bretschneider spectra.

In order to investigate any correlation between bimodality and the WPR in a quantitative manner it is first necessary to identify instances of double peaked spectra. Criteria for designing algorithms to detect these events using the confidence intervals of the wave spectrum have been outlined by a number of authors [17–19] while a simple and robust procedure—which has been used previously in the analysis of waves from Galway Bay—was developed by Barrett [3]. Following this methodology a spectral ordinate can be considered to be a valid secondary peak if:

— The peak is a local maximum
— If it has a magnitude of at least 15% of $S(f_{peak})$
— Separated from the primary peak (T_P) by a period of at least 2 seconds

This method was adapted in the analysis presented here so that various levels of 'multi-peakedness' could be discerned. A further criterion that the magnitude of the secondary peak must be a defined percentage (e.g. 115%) greater than the shallowest point of the trough separating it from the primary peak was introduced and the separating distance between the peaks was varied between 1 s to 5 s. The most stringent case—a secondary peak significantly larger than the trough and separated from the spectral peak by 5 s—selected a small number of instances which could be classed as 'extremely bimodal'.

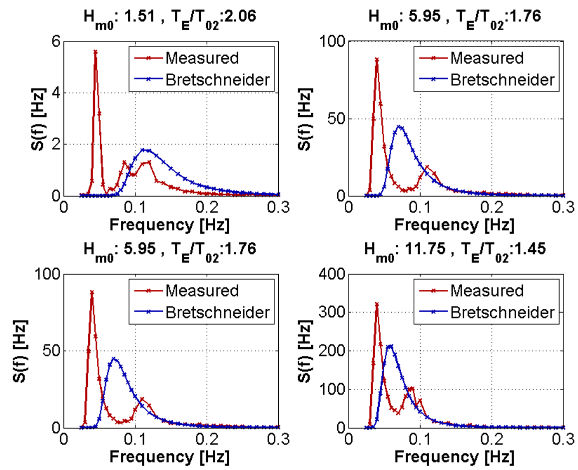

FIGURE 6. OUTLIER SPECTRA FROM FIGURE 2 PLOTTED AGAINST THEIR BRETSCHNEIDER EQUIVALENTS.

By applying this methodology to the data measured at AMETS in 2010 (13189 spectra) a series of groups of increasing multimodality were compiled. The method applied by Barrett identified 3723 cases at AMETS for the 2010 dataset, approximately 28% of measurements; this corresponds reasonably well with the work of Guedes Soares who showed that bimodal spectra composed 22% of observations at a North Atlantic location [17]. Separating the multimodal spectra from the general population allows Figure 2 to be redrawn in Figure 7. These spectra are shown to occur primarily during low sea-states (H_{m0} < 3 m) and display a higher WPR (1.352) than the remainder of the measurements (1.300). Single-peaked seas can be seen to account for many of the highest values of the WPR but also contribute most of the instances where the WPR approaches the value of 1.2 derived from the Bretschneider spectrum.

The average WPR for each of the groups of multi-peaked spectra are collated in Table 6. These results show that populations of spectra that have multiple peaks separated by longer and deeper troughs are shown to consistently display the highest average WPR values. The occurrence of a significant proportion of these spectral conditions within the AMETS dataset can be deemed at least partly responsible for the high average WPR, particularly among the low energy sea-states.

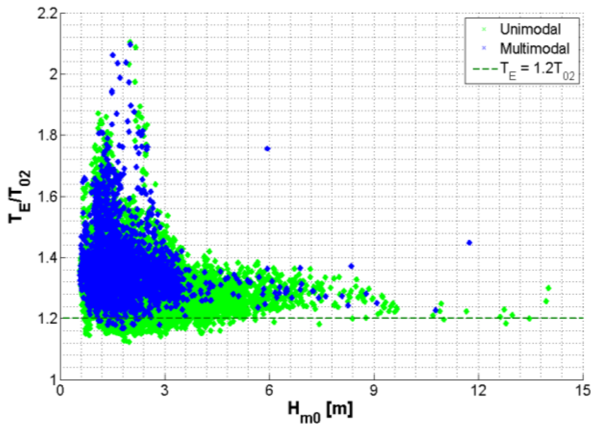

FIGURE 7. WAVE PERIOD RATIO PLOTTED AGAINST H_{M0} FOR UNIMODAL AND MULTIMODAL SEAS FOR AMETS (2010).

TABLE 6. AVERAGE WAVE PERIOD RATIOS FOR SELECTED GROUPS OF MULTIMODAL SPECTRA. NUMBER OF SPECTRA IN EACH GROUP INCLUDED IN BRACKETS.

Peak Separation [s]	Secondary Peak – Trough Difference				
	105%	110%	115%	120%	125%
1	1.350 *(4001)*	1.360 *(3048)*	1.368 *(2475)*	1.375 *(2075)*	1.381 *(1802)*
2	1.352 *(3723)*	1.363 *(2890)*	1.370 *(2389)*	1.376 *(2022)*	1.382 *(1769)*
3	1.365 *(2928)*	1.373 *(2413)*	1.378 *(2086)*	1.383 *(1829)*	1.387 *(1643)*
4	1.383 *(2083)*	1.391 *(1765)*	1.396 *(1556)*	1.400 *(1412)*	1.402 *(1305)*
5	1.409 *(1226)*	1.417 *(1059)*	1.422 *(959)*	1.426 *(887)*	1.428 *(838)*

Average Spectral Shape

Multimodal spectra represent explicit examples of deviation from the Bretschneider shape. Further analysis was carried out to assess the level of variation exhibited by the general population of data. Spectra from the 2010 AMETS, Umqua and Nantucket datasets with similar, and frequently occurring, summary statistics are grouped and plotted in Figures 8-10. The chosen sea states are as follows:

— 1.5 m < H_{m0} < 2 m, 4 s < T_{02} < 5 s
— 2 m < H_{m0} < 2.5 m, 5 s < T_{02} < 6 s
— 3 m < H_{m0} < 3.5 m, 6 s < T_{02} < 7 s
— 4 m < H_{m0} < 4.5 m, 7 s < T_{02} < 8 s

Sea-states were grouped using T_{02} rather than other alternative measures—T_E, T_p, T_{01} etc.—as this is the most commonly featured wave period parameter in the limited datasets that exist for the west coast of Ireland.

In Figures 8 & 9 all of the measured spectra that occurred within these ranges at each site are plotted, with the maximum and minimum spectral ordinate at each frequency component indicated by the solid black line. The average of the spectral ordinates is shown as the blue line and gives a general indication of the spectral shape that can be expected at each site. The equivalent Bretschneider spectrum that is also plotted is derived from calculating the spectral moments of the average spectrum and fitting the spectrum using the standard formula given by Tucker and Pitt [12]. Comparison between these two spectra indicates qualitatively how well the theoretical spectrum describes the real conditions at the various locations.

From visual inspection of Figures 8-10 it appears that the average spectra from Nantucket closely match the theoretical spectral shapes, though their peaks become more pronounced as H_{m0} increases. Measurements from this site had an average WPR of 1.205, similar to that derived for the Bretschneider Spectrum It is notable that while the average spectra from the AMETS and Umpqua datasets also display reasonable agreement with the general shape of their equivalent Bretschneider spectrum, they are shifted towards the lower frequency components. As with the cases of the multimodal spectra in the previous section this influences the derived spectral moments and results in a higher WPR. These plots also show that the resemblance of the average spectra to the equivalent Bretschneider shape is poor for the low sea-states at each site, while the greater sea-states exhibit good agreement. This corresponds well with the plot of WPR against H_{m0} at AMETS (Figure 1) where T_E/T_{02} approaches 1.2 more consistently as H_{m0} increased.

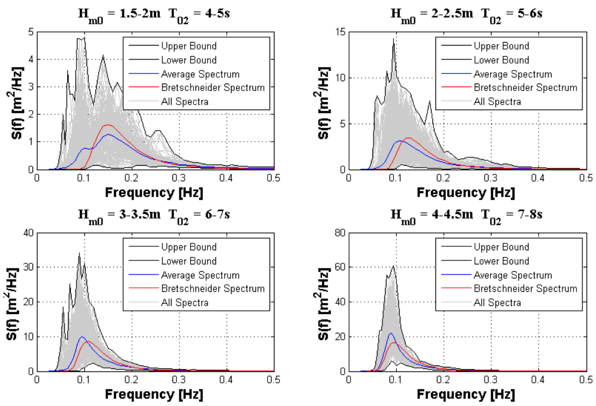

FIGURE 8. INDIVIDUAL, AVERAGE AND EQUIVALENT BRETSCHNEIDER SPECTRA FOR SELECTED SEA-STATES FROM AMETS.

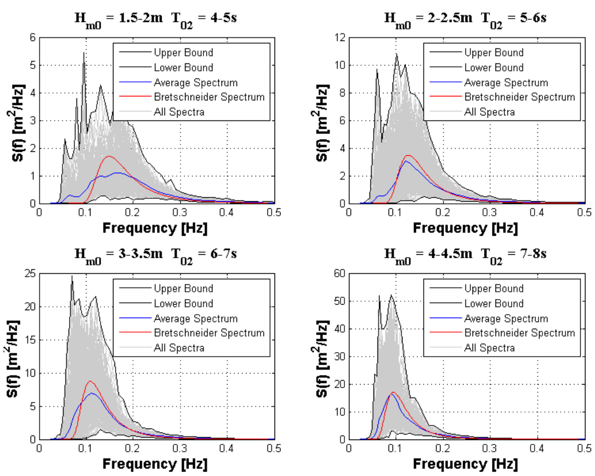

FIGURE 9. INDIVIDUAL, AVERAGE AND EQUIVALENT BRETSCHNEIDER SPECTRA FOR SELECTED SEA-STATES FROM UMPQUA.

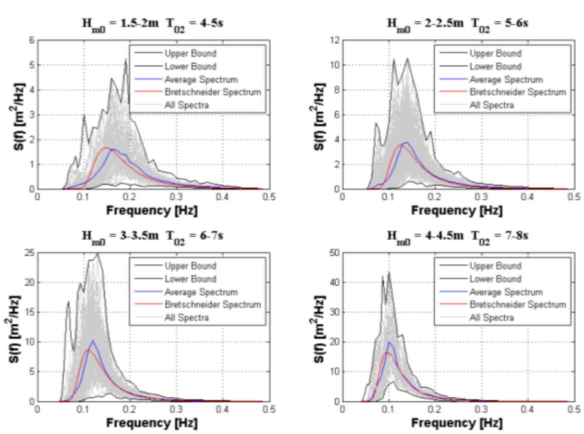

FIGURE 10. INDIVIDUAL, AVERAGE AND EQUIVALENT BRETSCHNEIDER SPECTRA FOR SELECTED SEA-STATES FROM NANTUCKET.

Spectral Fit

The level of fit between wave spectra has been computed in previous studies using a range of statistical tools. In this section the agreement that exists between the shapes of the measured spectra and their Bretschneider equivalents is investigated quantitatively using an error measures proposed by Sakhare and Deo [20], namely the commonly used correlation coefficient R. The calculation of R was limited to the frequency range $0.05Hz<f_p<0.2hz$, where f_p is the frequency of the maximum spectral ordinate, as components outside this range will tend to have little influence on the derived. Negative values of R are rare, but where they are detected they are seen to correspond to cases where a slight inverse relationship exists between the spectra, such as for bimodal spectra where the peak of the Bretschneider spectrum lies between the wind sea and swell components. Selected measured spectra from the AMETS dataset that display both high and low values of agreement with their equivalent Bretschneider spectra—defined by their R value—are presented in Figure 11.

More obvious trends are noticeable when individual values of the fit parameter R are plotted against the corresponding WPR in Figure 12. A color scale is also included in this figure as a means to highlight the density of occurrence of individual points within the center of the overall scatter. It can be seen that while many outliers exist, in general the spectra that have the best levels of fit with the Bretschneider spectrum tend to have the lowest ratios.

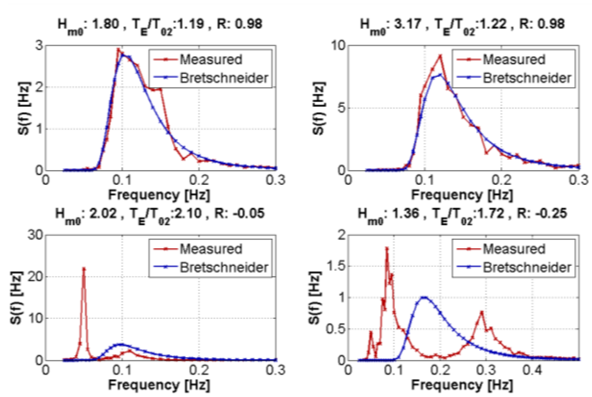

FIGURE 11. OUTLIER SPECTRA FROM FIG. 2 PLOTTED AGAINST THEIR BRETSCHNEIDER EQUIVALENTS.

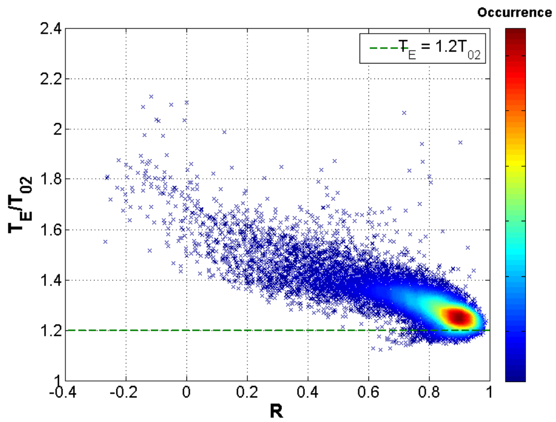

FIGURE 12. WAVE PERIOD RATIO PLOTTED AGAINST CORRELATION COEFFICIENT, R, FOR AMETS (2010).

Spectral Bandwidth

Spectral bandwidth is an important parameter for the representation of sea-states and is particularly useful in the study of spectral shape. In Figure 13 values of the WPR derived from observed spectra from the AMETS buoy are plotted against the corresponding bandwidth parameters ε_1 and ε_2 given by Equations 16-17. The values of these bandwidth parameters range from 0 to 1, with narrow banded spectra having the lowest values. For the theoretical Bretschneider Spectrum it can be shown that ε_1=.33 and ε_2=0.42.

$$\varepsilon_1 = \sqrt{\frac{m_1 m_{-1}}{\mathrm{m}_0^2} - 1} \qquad (16)$$

$$\varepsilon_2 = \upsilon = \sqrt{\frac{\mathrm{m}_0 \mathrm{m}_2}{\mathrm{m}_1^2} - 1} \qquad (17)$$

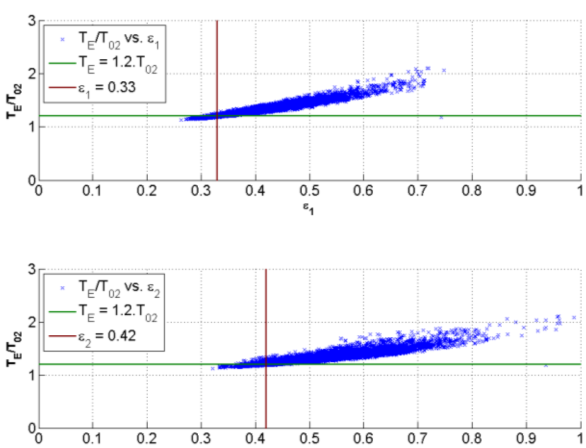

FIGURE 13. WAVE PERIOD RATIO PLOTTED AGAINST BANDWIDTH PARAMETERS ε_1 (TOP) AND ε_2 (BOTTOM) FOR AMETS (2010).

This figure displays a strong relationship between T_E/T_{02} and spectral bandwidth. It is noticeable that the narrowest spectra, i.e. those with values of ε_1 and ε_2 approaching 0, also tend to display the lowest T_E/T_{02} ratios. Conversely, the wide banded spectra account for the higher values of the WPR and mainly occur when H_{m0} is low, which agrees with the conclusions presented previously. This relationship would be a useful tool for selecting an appropriate WPR for different sea states—a linear best-fit line could be easily added to Figure 13—however in the majority of cases values of the bandwidth tend not to be supplied in the absence of spectral data.

These results also help confirm the suppositions drawn from the visual analysis of observed spectra in the previous sections. The averages of the measured spectra taken from the AMETS and Umqua buoy tend to contain additional low frequency components, leading to an increased spectral bandwidth and consequently a higher T_E/T_{02} than their Bretschneider equivalents, while the spectra observed at the Nantucket buoy were seen to be slightly narrower, with more pronounced peaks, though they still produced an average T_E/T_{02} of 1.21 which is close to what is expected from a Bretschneider spectrum. The combination of these studies provides a valuable insight into the importance of the dominant spectral shape in determining the relationship between T_E and T_{02} at a particular location.

CONCLUSIONS

This paper has defined a new parameter, the wave period ratio (WPR), and demonstrated that WPR values of 1.12 and 1.14 which have previously been employed in some studies are unrepresentative of either the Bretschneider or JONSWAP spectra. It has been shown that T_E=1.2T_{02} is the correct relationship if the Bretschneider shape is assumed to represent the sea-states, while for the most common JONSWAP form (γ=3.3) T_E=1.18T_{02} should be used to convert the zero-crossing period to the energy period for the calculation of wave power. Furthermore, the analysis of observed spectra indicates that the WPR is generally higher than these theoretical relationships for real sea conditions, depending on the geographical location and the prevailing wave climate. It has been shown that T_E is approximately equal to 1.32T_{02} off the West Coast of Ireland. If this ratio is assumed to be uniform off the Irish seaboard the value of the theoretical wave energy resource presented in the Irish Accessible Wave Energy Atlas should be revised upwards by 18%.

It has been also been shown that the relationship between T_E and T_{02} is heavily dictated by spectral shape. There is a close correlation between spectral bandwidth and the WPR, while it was also shown that degree to which sea-states' spectra conform to the Bretschneider formulation is generally indicative of the value of T_E/T_{02}. While the average spectral shapes at the Irish and US Pacific coasts show reasonable agreement with the equivalent Bretschneider spectra they can be seen to contain greater contributions from long period components, particularly for low sea-states. This deviation from the theoretical shape is compounded by the occurrence of multimodal spectra which contain both sea and swell inputs and which display high WPR values. As previous work has demonstrated, WPR will increase if the variance of the wave spectrum is shifted towards the lower frequencies [16]; this may explain why the WPRs at these locations were greater that the theoretical assumption.

In practice, to avoid errors associated with the variation in the WPR for real conditions, sea-state parameters should be derived directly from observed spectral data if available, rather than relying on archived summary statistics in isolation. It is recommended that an appropriate WPR should be calculated from measurements from a nearby buoy or wave model grid point if spectral data are unavailable at a location of interest, rather than assuming a value from a theoretical spectrum. The buoys near AMETS and Loop Head returned similar WPR values (1.32 and 1.33 respectively) despite their physical separation; a comparable value could be used to enhance the summary statistics provided by limited datasets off the Irish west coast such at the M-buoy network. Similarly, WPRs derived from the closest measurement buoy could be applied for the other regions analyzed in this paper; the US Atlantic coast, Oregon and California. This work has also highlighted the seasonal trends in the WPR, thus at least a full calendar years' worth of data should be analyzed to ensure an unbiased result.

ACKNOWLEDGEMENTS

This research was undertaken with the financial support of the Irish Research Council for Science Engineering and Technology (IRCSET) and the Science Foundation Ireland Charles Parsons Research Award. The Marine Institute and the Sustainable Energy Authority of Ireland (SEAI) are acknowledged for providing the ocean wave data from the Irish test sites required for this research.

REFERENCES

[1] ESB International, 2005, Accessible Wave Energy Resource Atlas, Marine Institute and Sustainable Energy Ireland.

[2] Glendenning I., and Count B. M., 1976, "Wave Power," Chem. Eng.

[3] Barrett S., 2010, "Floating Wave Energy Converters: Wave Measurement and Analysis Techniques," PhD, University College Cork.

[4] Dalton G. J., Alcorn R., and Lewis T., 2010, "Case study feasibility analysis of the Pelamis wave energy convertor in Ireland, Portugal and North America," Renew. Energy, **35**(2), pp. 443–455.

[5] Pitt E. G., Estimating power from wave measurements at the European Marine Energy Centre (EMEC) test site, Applied Wave Research.

[6] Crabb J. A., 1984, Assessment of Wave Power Available at Key United Kingdom Sites, Institute of Oceanographic Sciences.

[7] Cornett A. M., 2008, "A Global Wave Energy Resource Assessment," Proceedings of the Eighteenth International Offshore and Polar Engineering Conference, Vancouver, Canada.

[8] ABP Marine Environmental Research, 2008, Atlas of UK Marine Renewable Energy Resources: Technical Report, Department of Business, Enterprise and Regulatory Reform.

[9] European Marine Energy Centre (EMEC), 2009, Assessment of Wave Energy Resource.

[10] EquiMar Group, 2011, Wave and Tidal Resource Characterisation.

[11] IEC Technical Committee 114, Wave energy resource assessment and characterization (Draft).

[12] Tucker M. J., and Pitt E. G., 2001, Waves in ocean engineering, Elsevier.

[13] Det Norske Veritas, 2010, Environmental Conditions and Environmental Loads.

[14] Ochi M. K., 2005, Ocean Waves: The Stochastic Approach, Cambridge University Press.

[15] Holmes B., and Barrett S., 2007, "Sea and Swell Spectra," Porto, Portugal.

[16] Cahill B., 2013, "Characteristics of the wave energy resource at the Atlantic Marine Energy Test Site," PhD, University College Cork.

[17] Guedes Soares C., 1984, "Representation of double-peaked sea wave spectra," Ocean Eng., **11**(2), pp. 185–207.

[18] Guedes Soares C., 1991, "On the occurence of double peaked wave spectra," Ocean Eng., **18**(1–2), pp. 167–171.

[19] Rodríguez G., and Guedes Soares C., 1999, "A criterion for the automatic identification of multimodal sea wave spectra," Appl. Ocean Res., **21**(6), pp. 329–333.

[20] Sakhare S., and Deo M. C., 2009, "Derivation of wave spectrum using data driven methods," Mar. Struct., **22**(3), pp. 594–609.